

## Some Numerical Experiments Concerning Space-Time Reactor Kinetics Behavior

J. B. Yasinsky & A. F. Henry

**To cite this article:** J. B. Yasinsky & A. F. Henry (1965) Some Numerical Experiments Concerning Space-Time Reactor Kinetics Behavior, Nuclear Science and Engineering, 22:2, 171-181, DOI: [10.13182/NSE65-A20236](https://doi.org/10.13182/NSE65-A20236)

**To link to this article:** <https://doi.org/10.13182/NSE65-A20236>



Published online: 12 May 2017.



Submit your article to this journal [↗](#)



Article views: 45



View related articles [↗](#)



Citing articles: 1 View citing articles [↗](#)

## Some Numerical Experiments Concerning Space-Time Reactor Kinetics Behavior\*

J. B. Yasinsky and A. F. Henry

*Bettis Atomic Power Laboratory, Westinghouse Electric Corporation, West Mifflin, Pennsylvania 15122*

*Received October 2, 1964*

*Revised January 25, 1965*

Numerical comparisons have been made between exact and approximate solutions to the two-group space-time diffusion equations. Two slab cores were studied, one 240-cm thick and the other 60-cm thick. Prompt critical bursts and limited ramp insertions of reactivity were simulated by imposing perturbations on the fission cross sections throughout the first quarter of the core. Feedback effects were neglected. Results were obtained using the conventional point kinetics equation, the adiabatic approximation and the space-time synthesis method. For one situation, two nodal methods were also examined. Comparisons with the exact space-time solutions suggest that, when the point kinetics equations are expected on qualitative grounds to be a poor approximation, the actual quantitative errors can be extremely large. Of the other approximations tested the space-time synthesis method gave the most accurate results.

### INTRODUCTION

It is well known that the conventional 'point' reactor kinetics equations (Eq. (3) below) become suspect for certain transients in large reactors. This is because these equations, as generally used, are based on the assumption that the flux shape (as distinct from its amplitude) remains constant during the transient<sup>1</sup>. In a rigorous formulation, reactivity is determined by this flux shape. Hence, for a given perturbation the solution to the kinetics equations can change (sometimes substantially) if flux shape changes are taken into account.

It is not clear exactly when the point kinetics equations become seriously in error. Qualitatively, large perturbations in nuclearly large cores are the ones most likely to require more elaborate analysis. Small 'tightly coupled' cores are expected to be well described by conventional methods. But quantitative information concerning the magnitude of errors and the conditions which lead to them has not been generally available.

With the development of computer programs capable of solving the space-time diffusion equa-

tions in detail<sup>2,3,4</sup> a more precise evaluation of the accuracy of the point kinetics equations is becoming possible. The present paper describes such a study for two very simple slab cores having material compositions typical of light water-moderated power reactors. The first core (240-cm thick) is representative of a large loosely coupled reactor. The second (60-cm thick) would generally be thought of as tightly coupled.

In the numerical experiments to be presented, both of these reactors, initially critical, were perturbed by certain local changes in fission cross sections in such a manner as to accentuate non-separable space-time effects. The resulting transients were described 'exactly' by WIGLE<sup>5</sup>, a

---

<sup>2</sup>R. E. TILLER and C. A. OSTER, "CLUMSY-I—A Time and Space Dependent Reactor Kinetics Code for the IBM-7090 Computer," HW-77221.

<sup>3</sup>A. R. CURTIS, J. G. TYROR and H. E. WRIGLEY, "STAB—A Kinetic Three-Dimensional One-Group Digital Computer Program," AEEWR 77 (1961).

<sup>4</sup>J. W. RIESE, "VARIQUIR—A Two-Dimensional Time Dependent Multigroup Diffusion Code," WANL-TNR-133 (1963).

<sup>5</sup>W. R. CADWELL, A. F. HENRY and A. J. VIGIOTTI, "WIGLE—A Program for the Solution of the Two-Group Space-Time Diffusion Equations in Slab Geometry," WAPD-TM-416 (1964).

\*Work performed under the auspices of the USAEC.

<sup>1</sup>A. F. HENRY, *Nucl. Sci. Eng.*, 3, 52 (1958).

two-energy-group space-time diffusion-theory program in which all coefficients (diffusion constants, cross sections, etc.) can be varied linearly in time. The same transients were analyzed by conventional perturbation theory, and in addition by the so-called 'adiabatic' approximation, by a flux synthesis technique and (for one example) by two nodal methods. Since the version of WIGLE used has no capability to describe feedback effects, the results are unrealistic from a physical point of view. However, this very lack of feedback permits distinguishing between situations where the space-time description is intrinsically accurate and those where it is poor but unimportant. (Prompt critical excursions, having periods of a few milliseconds prior to termination, usually end when a certain amount of energy has been released. When this energy feedback is made predominant in the mathematical model of the excursion, predictions become much less sensitive to the accuracy with which the neutron kinetics are described.) One definite advantage of using WIGLE as a standard was that it is quite fast. (Running time for a typical two-neutron-group, one-delayed-group, 50-mesh-point problem involving 400 time steps is 0.9 min on a Philco 2000.)

In the sections below we first review the theory of the point kinetics, adiabatic, synthesis and nodal approximations. Problems and results are then described for both prompt critical and moderate (ramp reactivity) excursions. Since the detailed space-time solutions are available we also show some comparison between the amplitude function of the kinetics equations ( $T$  of Eq. (2)), the actual reactor power level and the reading of a local counter.

### THEORY

If fuel is stationary and all feedback effects are neglected, the time-dependent, two-group diffusion-theory representation of a reactor in the absence of external sources is

$$\left. \begin{aligned} \nabla \cdot D_1 \nabla \phi_1 - \Sigma_1 \phi_1 + (1 - \beta) [\nu \Sigma_{f_1} \phi_1 + \nu \Sigma_{f_2} \phi_2] + \sum_i \lambda_i c_i &= v_1^{-1} \dot{\phi}_1 \\ \nabla \cdot D_2 \nabla \phi_2 - \Sigma_2 \phi_2 + \Sigma_{R_1} \phi_1 &= v_2^{-1} \dot{\phi}_2 \\ \beta_i [\nu \Sigma_{f_1} \phi_1 + \nu \Sigma_{f_2} \phi_2] - \lambda_i c_i &= \dot{c}_i \end{aligned} \right\} \quad (1)$$

where  $D_i$ ,  $\Sigma_i$ ,  $\Sigma_{f_i}$  and  $\Sigma_{R_i}$  stand for the diffusion constant, removal plus absorption, fission and removal cross sections of the  $i$ 'th group with subscripts  $i = 1$  and 2 referring to fast and thermal groups. With the definitions

$$T \equiv \int (\psi_1^* v_1^{-1} \phi_1 + \psi_2^* v_2^{-1} \phi_2) dV; \quad C_i = \int \psi_i^* c_i dV, \quad (2)$$

where  $\psi_1^*$  and  $\psi_2^*$  are the fast and thermal unperturbed adjoint fluxes, the standard kinetics equations become<sup>1</sup>

$$\left. \begin{aligned} \dot{T} &= \frac{\rho - \bar{\beta}}{\Lambda} T + \sum_i \lambda_i C_i \\ \dot{C}_i &= -\lambda_i C_i + \frac{\bar{\beta}_i}{\Lambda} T \end{aligned} \right\} \quad (3)$$

These follow directly from adjoint weighting and subsequent integration of Eqs. (1).

If the reactor is perturbed from its critical state by changes in the fission cross sections only, the expressions for reactivity,  $\rho$ , and prompt-neutron life-time,  $\Lambda$ , become

$$\rho = \frac{\int \psi_1^*(\mathbf{r}) \delta(\nu \Sigma_{f_1}) \psi_1(\mathbf{r}, t) dV + \int \psi_1^*(\mathbf{r}) \delta(\nu \Sigma_{f_2}) \psi_2(\mathbf{r}, t) dV}{\int \psi_1^*(\mathbf{r}) \nu \Sigma_{f_1} \psi_1(\mathbf{r}, t) dV + \int \psi_1^*(\mathbf{r}) \nu \Sigma_{f_2} \psi_2(\mathbf{r}, t) dV} \quad (4)$$

$$\Lambda = \frac{\int \psi_1^*(\mathbf{r}) v_1^{-1} \psi_1(\mathbf{r}, t) dV + \int \psi_2^*(\mathbf{r}) v_2^{-1} \psi_2(\mathbf{r}, t) dV}{\int \psi_1^*(\mathbf{r}) \nu \Sigma_{f_1} \psi_1(\mathbf{r}, t) dV + \int \psi_1^*(\mathbf{r}) \nu \Sigma_{f_2} \psi_2(\mathbf{r}, t) dV}, \quad (5)$$

where  $\psi_1(\mathbf{r}, t)$  and  $\psi_2(\mathbf{r}, t)$  are fast and thermal time-dependent shape functions defined as

$$\psi_1(\mathbf{r}, t) = \phi_1(\mathbf{r}, t)/T(t); \quad \psi_2(\mathbf{r}, t) = \phi_2(\mathbf{r}, t)/T(t).$$

Unfortunately, the expressions (4) and (5) can be used in their above form only if one has a preceding knowledge of the true space-time flux. For this reason certain approximate methods have been developed in order to describe kinetic behavior.

### 1. The Conventional Point Kinetics Method

This method is the standard approximation. In it one assumes that the flux shape is unaffected by any reactor perturbation so that

$$\phi_1(\mathbf{r}, t) = T(t) \psi_1(\mathbf{r}) \quad \text{and} \quad \phi_2(\mathbf{r}, t) = T(t) \psi_2(\mathbf{r}), \quad (6)$$

where  $\psi_1(\mathbf{r})$  and  $\psi_2(\mathbf{r})$  are the unperturbed fast and thermal flux shapes. The amplitude function  $T(t)$  is obtained by solving Eqs. (3) where  $\rho$  and  $\Lambda$  have been calculated by replacing  $\psi_1(\mathbf{r}, t)$  and  $\psi_2(\mathbf{r}, t)$  in Eqs. (4) and (5) by  $\psi_1(\mathbf{r})$  and  $\psi_2(\mathbf{r})$ . Since this method is insensitive to any change in the flux shape, it can be expected to yield adequate results only when flux tilting is absent or small.

### 2. The Adiabatic Approximation<sup>6</sup>

This method assumes that at every instant during a transient, the flux shape can be obtained by

<sup>6</sup>A. F. HENRY and N. J. CURLEE, *Nucl. Sci. Eng.*, **4**, 727 (1958).

static calculations. The space-time flux is then represented by

$$\phi_1(\mathbf{r}, t) = T(t)\psi_1'(\mathbf{r}) \quad \text{and} \quad \phi_2(\mathbf{r}, t) = T(t)\psi_2'(\mathbf{r}), \quad (7)$$

where  $\psi_1'(\mathbf{r})$  and  $\psi_2'(\mathbf{r})$  are the fast and thermal flux shapes resulting from a static calculation at time  $t$ . In this case the true time-dependent flux shapes appearing in the expressions for  $\rho$  and  $\Lambda$  are approximated by  $\psi_1'(\mathbf{r})$  and  $\psi_2'(\mathbf{r})$ .

### 3. The Multimode Synthesis Method<sup>7</sup>

The two-group flux vector in this approximation is represented as

$$\Phi(\mathbf{r}, t) = \begin{pmatrix} \phi_1(\mathbf{r}, t) \\ \phi_2(\mathbf{r}, t) \end{pmatrix} = \sum_{i=1}^k T_i(t) \begin{pmatrix} \psi_1(\mathbf{r}) \\ \psi_2(\mathbf{r}) \end{pmatrix}_i = \sum_{i=1}^k T_i(t) \Psi_i(\mathbf{r}), \quad (8)$$

where the  $T_i(t)$  are scalar mixing coefficients and the  $\Psi_i(\mathbf{r})$  are known spatial flux vectors representative of reactor conditions at various times during a transient. The  $k$  amplitude functions are found by solving the set of  $k$ 'th order matrix equations, analogous to the scalar Eqs. (3), which result when Eq. (8) is substituted into Eq. (1), weighted by adjoint vectors  $\Psi_i^*(\mathbf{r})$  and integrated over the reactor space.

It should be noted that a great deal more freedom is possible in choosing the trial vectors  $\Psi_i(\mathbf{r})$  in the multimode synthesis method than in choosing the vectors  $\Psi'(\mathbf{r})$  in the adiabatic approximation. For the latter approximation to be accurate,  $\Psi'(\mathbf{r})$  at time  $t$  must be close in shape to the exact solution vector  $\Psi(\mathbf{r}, t)$ . Unfortunately even if the exact physical conditions of the reactor throughout the transient are known a priori,  $\Psi'(\mathbf{r})$ , computed as it is by static methods, is frequently a poor approximation to  $\Psi(\mathbf{r}, t)$ . When feedback effects enter the picture (so that the reactor conditions at time  $t$  are *not* known a priori) the approximation frequently becomes completely invalid. On the other hand, all that is required of the  $\Psi_i(\mathbf{r})$  is that linear combinations of them be a good approximation to  $\Psi(\mathbf{r}, t)$  throughout the transient. Even with feedback present it is possible beforehand to make reasonable estimates of reactor conditions which bracket those actually to be experienced. Linear combinations of static shapes associated with these estimated conditions can generally pro-

vide a good approximation to  $\Psi(\mathbf{r}, t)$ . If not, a single iteration in which the first approximation to the reactor conditions during the transient is used as a basis for determining an improved set of trial functions ought to provide the necessary improvement.

The question of how many trial functions to use in the multimode approximation is frequently very disturbing to those who have had no experience with the method. In practice the number must be obtained empirically by comparison with more accurate calculations for the case at hand or by adding more trial functions and seeing if any difference results. The situation is quite analogous to the choice of the number of groups or the group cut points in a few-group scheme. For one-dimensional cases comparisons with multigroup computations serve to justify the few-group structure selected. This same structure is then used in multidimensional cases where comparison with multigroup results cannot be made.

### 4. Nodal Methods

#### a) Gross Coupling Method<sup>8,9</sup>

The nodal technique consists of dividing the reactor volume,  $R$ , into subregions or nodes,  $V_i$ , in each of which the time behavior of some average flux is determined. The nodal equations are obtained by integrating the diffusion equations over each node and defining an average nodal flux

$$\phi_i = \frac{1}{V_i} \int_{R_i} \phi dR \quad (9)$$

and the average nodal material parameters. The essential assumption of the gross coupling scheme is that the gross current from node  $i$  to node  $j$  is proportional to the average flux in node  $i$ ; that is,

$$j_{ij}^+ = p_{ij} V_i \phi_i. \quad (10)$$

For diffusion theory

$$p_{ij} = \frac{1}{V_i \psi_i} \left[ \frac{1}{4} \oint_{S_{ij}} \psi dS - \frac{1}{2} \oint_{S_{ij}} D \nabla \psi \cdot N_i dS \right], \quad (11)$$

where the  $\psi_i$  are average fluxes resulting from a static calculation of the unperturbed system. The resulting  $i$ 'th node equations for two-energy groups with no delayed neutrons are

<sup>8</sup>S. KAPLAN, R. EWEN, N. J. CURLEE and S. MARGOLIS, *Space-Time Kinetics*, Section 5.4, Naval Reactors Physics Handbook (1962).

<sup>9</sup>E. L. WACHSPRESS, R. D. BURGESS and S. BARON, *Nucl. Sci. Eng.*, 12, 381-389 (1962).

<sup>7</sup>S. KAPLAN, O. J. MARLOWE and J. BEWICK, *Nucl. Sci. Eng.*, 18, 163 (1964).

$$\left. \begin{aligned} - \left[ \sum_j p_{ij}^F + \Sigma_i^F \right] V_i \phi_i^F + \sum_j p_{ji}^F V_j \phi_j^F + \nu \Sigma_{fi}^F V_i \phi_i^F + \nu \Sigma_{fi}^S V_i \phi_i^S &= 1/v^F V_i \dot{\phi}_i^F \\ - \left[ \sum_j p_{ij}^S + \Sigma_i^S \right] V_i \phi_i^S + \sum_j p_{ji}^S V_j \phi_j^S + \Sigma_{Ri}^F V_i \phi_i^F &= 1/v^S V_i \dot{\phi}_i^S \end{aligned} \right\} \quad (12)$$

### b) The Effective $D/L$ Method

This method is similar to a course finite difference approach. It consists of integrating the diffusion equations over each node and defining average parameters and average fluxes that are located at the center of each node. The net current between the  $i$ 'th and the  $j$ 'th node is then approximated by

$$j_{ij} = - \frac{\tilde{D}_{ij}}{L_{ij}} (\phi_j - \phi_i) S_{ij}, \quad (13)$$

where  $S_{ij}$  is the area of the  $i, j$  interface,  $L_{ij}$  is the distance from the center of the  $i$ 'th node to the center of the  $j$ 'th node, and  $\tilde{D}_{ij}$  is an effective diffusion coefficient. For the present study the  $\tilde{D}_{ij}$  were found by multiplying the volume-averaged diffusion constants for each nodal zone by a factor which was adjusted so that the few-node fundamental eigenvalue was the same as that of an unperturbed fine-mesh problem. For two-energy groups with no delayed neutrons the  $i$ 'th node equations are

TABLE I  
Material Parameters for Critical Cores

	240-cm core	60-cm core
$D_1$ (cm)	1.69531	1.69531
$D_2$ (cm)	0.409718	0.409718
$\Sigma_{a1}$ (cm $^{-1}$ )	0.0137513	0.0137513
$\Sigma_{a2}$ (cm $^{-1}$ )	0.261361	0.261361
$\Sigma_{r1}$ (cm $^{-1}$ )	0.0164444	0.0164444
$\nu \Sigma_{f1}$ (cm $^{-1}$ )	0.0194962	0.0213143
$\nu \Sigma_{f2}$ (cm $^{-1}$ )	0.497857	0.544286
$B_T^2$ (region 1) (cm $^{-2}$ )	0.0109100	0.0109100
$B_T^2$ (region 2) (cm $^{-2}$ )	0.0120000	0.0120000
$B_T^2$ (region 3) (cm $^{-2}$ )	0.0108900	0.0108900

$$\left. \begin{aligned} - \left[ S_{i,i+1} \frac{\tilde{D}_{i,i+1}^F}{L_{i,i+1}} + S_{i,i-1} \frac{\tilde{D}_{i,i-1}^F}{L_{i,i-1}} + \Sigma_i^F V_i - \nu \Sigma_{fi}^F V_i \right] \phi_i^F + S_{i,i-1} \frac{\tilde{D}_{i,i-1}^F}{L_{i,i-1}} \phi_{i,i-1}^F + S_{i,i+1} \frac{\tilde{D}_{i,i+1}^F}{L_{i,i+1}} \phi_{i,i+1}^F + \nu \Sigma_{fi}^S V_i \phi_i^S \\ = 1/v_i^F V_i \dot{\phi}_i^F \\ - \left[ S_{i,i+1} \frac{\tilde{D}_{i,i+1}^S}{L_{i,i+1}} + S_{i,i-1} \frac{\tilde{D}_{i,i-1}^S}{L_{i,i-1}} + \Sigma_i^S V_i \right] \phi_i^S + S_{i,i-1} \frac{\tilde{D}_{i,i-1}^S}{L_{i,i-1}} \phi_{i,i-1}^S + S_{i,i+1} \frac{\tilde{D}_{i,i+1}^S}{L_{i,i+1}} \phi_{i,i+1}^S + \Sigma_{Ri}^F V_i \phi_i^F = 1/v_i^S V_i \dot{\phi}_i^S \end{aligned} \right\} \quad (14)$$

### PROBLEMS

To test the applicability of point kinetics equations and the other approximations discussed above, two one-dimensional bare cores were subjected to prompt and delayed supercritical excursions chosen to accentuate nonseparable space-time effects. The two cores, one 240-cm and the other 60-cm thick, consisted of three regions, uniform in material composition, except for region-dependent transverse bucklings. The critical material parameters for the two cores, typical of light water-moderated power reactors, are given in Table I.

Each of these cores was subjected first to a prompt critical transient, of duration 0.01 sec, during which the effects of the delayed neutrons were neglected because of the short transient time. The perturbation from critical consisted of step increases of  $\nu \Sigma_{f1}$  and  $\nu \Sigma_{f2}$  in the first quarter (region-1) of each core, followed by a decreasing ramp of the same parameters for 0.01 sec. The maximum and minimum values of reactivity during the transient were about  $\pm 2\%$  as calculated by perturbation theory. The initial and final values of the region-1 perturbed fission cross sections used in this problem appear in Table II.

TABLE II  
Region-1 Perturbed Fission Cross Sections  
for Prompt Critical Transient Problems

Time sec	240-cm core		60-cm core	
	$\nu\Sigma_{f1}$ (cm <sup>-1</sup> )	$\nu\Sigma_{f2}$ (cm <sup>-1</sup> )	$\nu\Sigma_{f1}$ (cm <sup>-1</sup> )	$\nu\Sigma_{f2}$ (cm <sup>-1</sup> )
0+	0.0213561	0.545353	0.0257143	0.656644
0.01	0.0176363	0.450361	0.0169143	0.431928

The second transient problem was an excursion in the range above critical but below prompt critical. Each core was perturbed from its critical state by increasing fission cross sections in region 1 in a ramp fashion (from 0 to 0.8 sec in the case of the 240-cm core, and from 0 to 1.0 sec for the 60-cm core). The cross sections were then held constant until  $t = 100$  sec. The reactivity in both cases of this problem was always less than prompt critical (i.e.,  $\rho < \beta$ ). One group of delayed neutron precursors was considered with the effective delayed neutron fraction  $\beta = 0.0064$  and the effective decay constant  $\lambda = 0.08 \text{ sec}^{-1}$ . The region-1 perturbed fission cross sections for this problem are given in Table III.

All of these transients are asymmetric and most of them involve local perturbations which are large compared to the overall leakage. Thus space-time effects are definitely expected. Our primary concern is with the magnitude of these effects.

## RESULTS

### 1. Prompt Critical Transient

Both cores were perturbed throughout region 1 as described above, and solutions of the time-dependent diffusion Eqs. (1) were obtained from WIGLE<sup>5</sup>. Time increments of  $5 \times 10^{-6}$  sec were found to be sufficient to yield accurate results, and 12 spatial mesh points were employed. Also, throughout this study the fast inverse velocity,

$v_1^{-1}$ , was set equal to zero to prevent the necessity of using even smaller time steps in the solution of the time-dependent diffusion equations. The thermal velocity,  $v_2$ , was chosen to be  $2.2 \times 10^5$  cm/sec. The fluxes  $\phi_1(x, t)$  and  $\phi_2(x, t)$  thus obtained were considered as exact values to which the approximate results could be compared. In Figs. 1 and 2, the fast flux,  $\phi_1(x, t)$ , is shown for the two cores at several instants during the transient. The very sizeable flux tilt in the loosely coupled core is evident (Fig. 1). For the 60-cm core, tilting is much less.

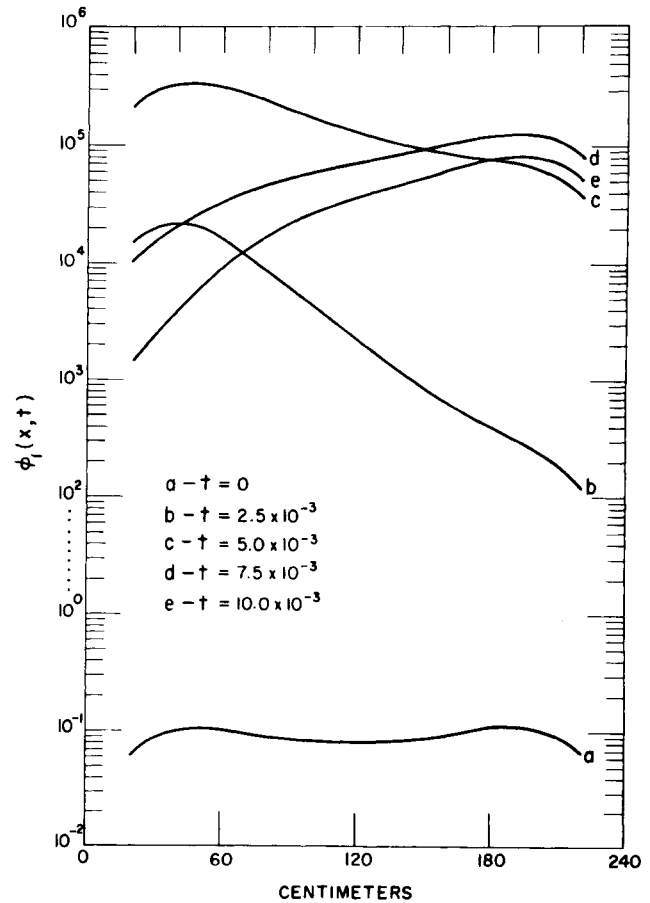


Fig. 1. Spatial fast flux (240 cm core).

TABLE III  
Region-1 Perturbed Fission Cross Sections  
for Delayed Critical Transient Problems

240-cm core			60-cm core		
Time sec	$\nu\Sigma_{f1}$ (cm <sup>-1</sup> )	$\nu\Sigma_{f2}$ (cm <sup>-1</sup> )	Time sec	$\nu\Sigma_{f1}$ (cm <sup>-1</sup> )	$\nu\Sigma_{f2}$ (cm <sup>-1</sup> )
0.0	0.0194962	0.497852	0.0	0.0213143	0.544286
0.8	0.0197343	0.503936	1.0	0.0220224	0.562367
100	0.0197343	0.503936	100	0.0220224	0.562367

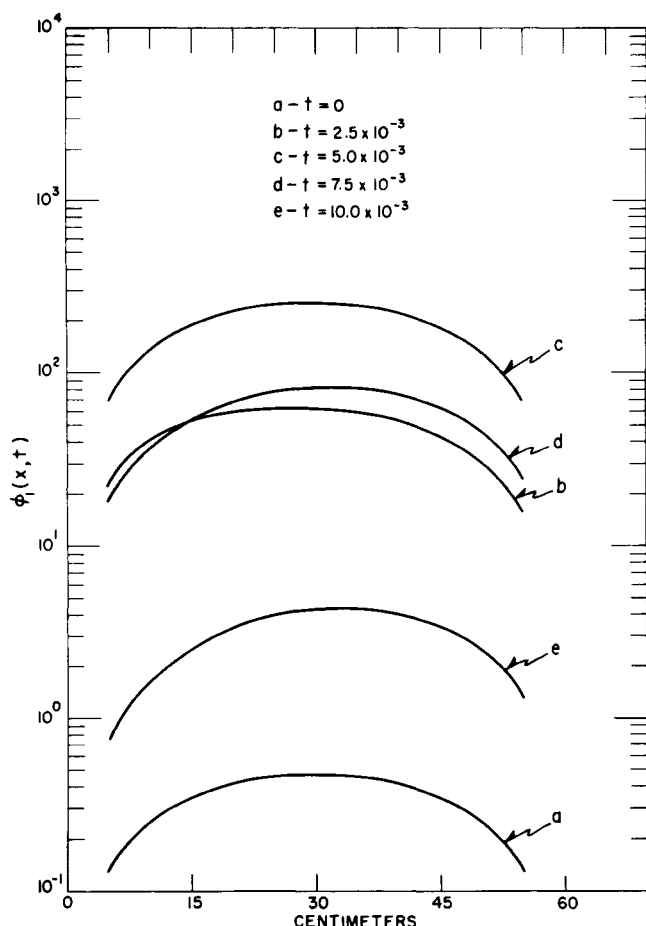


Fig. 2. Spatial fast flux (60 cm core).

Using the exact fluxes and the perturbed fission cross sections of Table II, the exact time variation of the reactivity,  $\rho$ , and the prompt neutron lifetime,  $\Lambda$ , were obtained from Eqs. (4) and (5) for both cores. With  $\rho/\Lambda$  known as a function of time, the kinetics Eqs. (3) were then solved<sup>a</sup> and the amplitude function  $T(t)$  obtained. With proper normalization,  $T(t)$  obtained in this manner must (and did) agree with the direct definition (Eqs. (2)). The time-dependent shape functions  $\psi_1(x, t)$  and  $\psi_2(x, t)$  were then calculated from the ratios of the true space-time fluxes and the amplitude function. Thus, the exact solution was obtained in the form  $\phi(x, t) = T(t)\psi(x, t)$ .

With  $\phi(x, t)$  known exactly this entire manipulation is of course just an exercise. It does, however, verify that if 'exact' (i.e. Eqs. (4) and (5)) values of  $\rho$  and  $\Lambda$  are known, the amplitude function, as described by Eq. (2), does indeed result from a solution of the kinetics equations. Also, it casts the exact solution into the same form (product of an amplitude and a shape) as that which

of necessity results from application of the point or adiabatic approximations. We thus shall be able to use the values of  $\rho(t)$  and  $T(t)$  determined by these approximations as a measure of their accuracy.

The other approximations previously described were next applied. Conventional point kinetics results and the adiabatic approximation results were obtained as discussed in the section on Theory. In the adiabatic case the required flux shapes, obtained from static WANDA calculations<sup>10</sup> at several instants during the transient, were normalized such that

$$\frac{\int \psi_2^*(x) v_2^{-1} \psi_2^t(x) dx}{\int \psi_2^*(x) v_2^{-1} \psi_2^0(x) dx} = 1. \quad (15)$$

The time-dependent normalization is necessary if the kinetics Eqs. (3) are to be of the form given<sup>1</sup>. Equation (15) also implies that  $T(0) = 1$ ; we have normalized all results in this manner.

In applying the multimode synthesis method, two trial functions were used initially for both cores, the first representing the initial unperturbed conditions and the second representative of the perturbed conditions at 2.5 msec. The mixing coefficients  $T_1(t)$  and  $T_2(t)$  were obtained by solving<sup>b</sup> the matrix equation

$$\begin{bmatrix} \rho_{11} & \rho_{12} \\ \rho_{21} & \rho_{22} \end{bmatrix} \begin{bmatrix} T_1 \\ T_2 \end{bmatrix} = \begin{bmatrix} v_{11}^{-1} & v_{12}^{-1} \\ v_{21}^{-1} & v_{22}^{-1} \end{bmatrix} \begin{bmatrix} \dot{T}_1 \\ \dot{T}_2 \end{bmatrix}, \quad (16)$$

which results when the form (8) is inserted into Eq. (1), weighted by the adjoint functions corresponding to the  $\Psi_i(r)$ , and integrated. The elements  $\rho_{ij}$  vary with time since the weighted integrals of the fission cross sections are time-dependent. For the 240-cm core, results obtained from two trial functions were quite inaccurate. Accordingly, a third trial function representing conditions at 7.5 msec was chosen for the larger core, and the three mixing coefficients  $T_1(t)$ ,  $T_2(t)$  and  $T_3(t)$  were then obtained from the third-order version of Eq. (16). (As explained earlier, had the exact solution not been available, we should have chosen the number of trial functions simply by starting with two and increasing the number until no significant change was expected from further addition.)

For the point and adiabatic approximations the reactivity and resulting amplitude function are

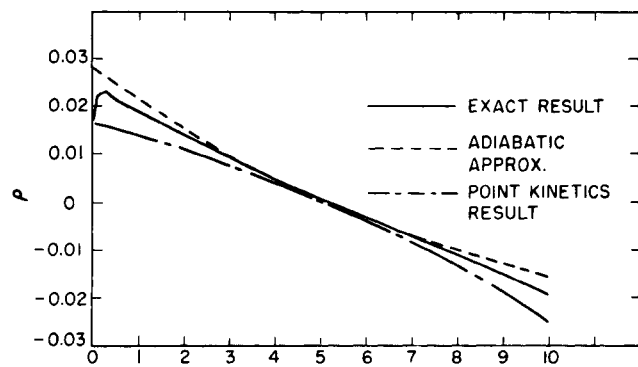
<sup>b</sup>An experimental program for solving these equations was provided by W. G. Clarke.

<sup>a</sup>An experimental digital program created by M. A. Pulick and W. G. Clarke was used for this purpose.

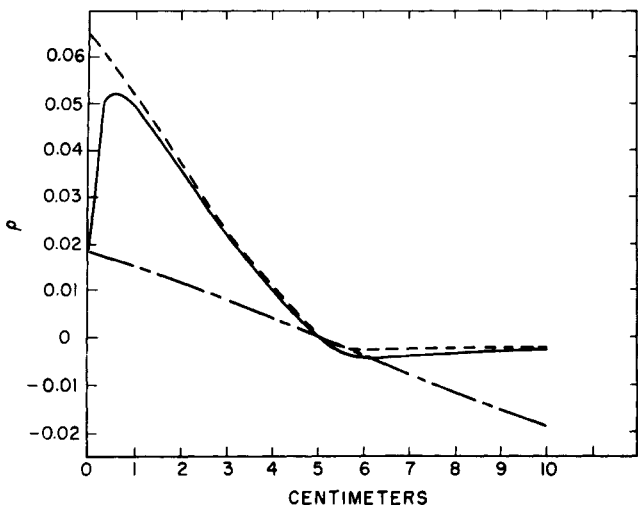
<sup>10</sup>O. J. MARLOWE and M. C. SUGGS, "WANDA-5-A One-Dimensional Neutron Diffusion Equation Program for the Philco-2000 Computer," WAPD-TM-241 (1960).

obtained as essential parts of the computation. Comparison with these same quantities as predicted by the exact solution then provides a measure of the adequacy of the approximations. Such a comparison is shown in Figs. 3, 4 and 5.

Figure 3 shows reactivity as a function of time for the two cores. The magnitude of the inadequacy of the point approximation is striking, particularly for the large core. The difference results of course from the tilting of the flux shape into a region where the fission cross section has just been increased. (Because of this tilting, the exact reactivity actually increases during a time when the only perturbation is a continuous decrease in fission cross section.) In the point case, since the unperturbed shape is used to compute  $\rho$ , no effect of tilting is observed. Instead, because of the linear decrease in fission cross section following the initial step increase,  $\rho(t)$  falls off approximately linearly. (Because the denominator of Eq. (4) contains the perturbed, time-dependent fission



a) for a 60-cm core



b) for a 240-cm core.

Fig. 3. Time behavior of reactivities.

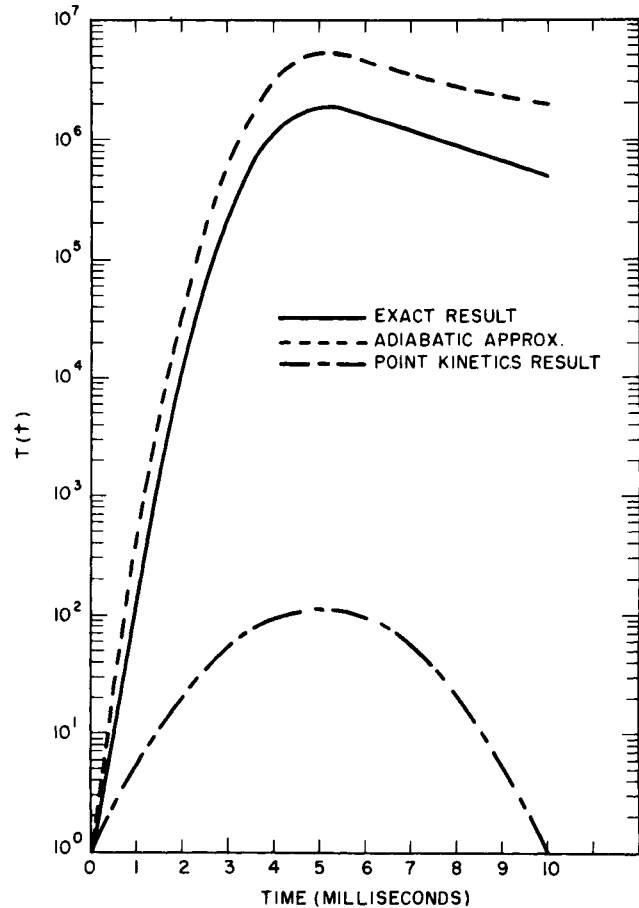


Fig. 4. Prompt critical excursion amplitude function  $T(t)$  for 240 cm core.

cross section, the falloff is not exactly linear.) Since in the adiabatic approximation the flux shape assumes an asymptotic value instantly, the tilting at time  $0^+$  is exaggerated, and the adiabatic value of  $\rho$  exceeds the exact result.

As is to be expected from the reactivity behavior, the amplitude function predicted for these transients is in considerable error. This is particularly true for the point approximation. In fact for the large core, Fig. 4 shows that the point approximation underestimates the maximum amplitude of the excursion by a factor of over  $10^4$ . Even for the tightly coupled (60-cm) core (Fig. 5), it underestimates the maximum by a factor of 4. Figures 4 and 5 also show predictions of the adiabatic approximation. There is slight improvement in the small core and a major improvement in the large one. The fact that the adiabatic approximation overestimates the amplitude of the excursion is consistent with the corresponding reactivity behavior (Fig. 3). Since no power-induced feedback is present in the model being examined, these results are not realistic physically. Nevertheless, the fact that the error in the conventional point method is intrinsically so great



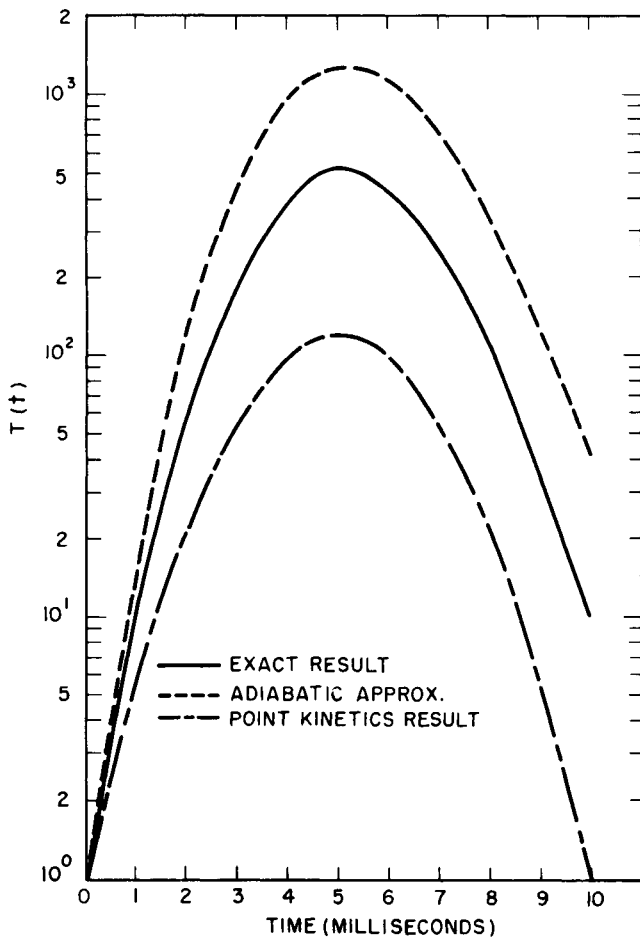


Fig. 5. Prompt critical excursion amplitude function  $T(t)$  for 60 cm core.

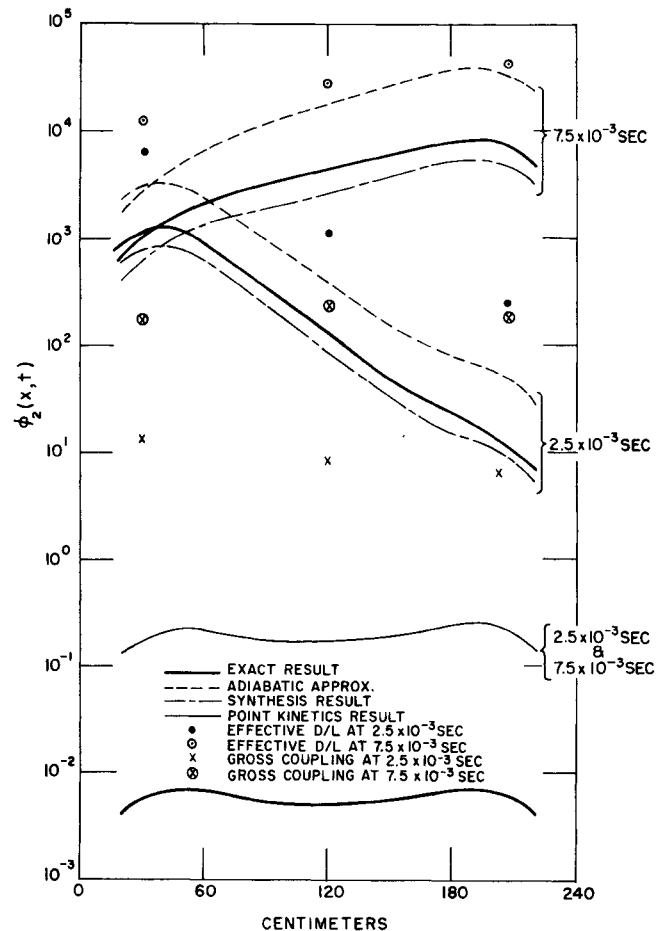


Fig. 6. Prompt critical excursion thermal flux at various times for 240 cm core.

for the large core lends considerable support to the view that this model should never be used to analyze prompt excursions in large reactors.

Figure 6 shows for the 240-cm core a comparison of predicted thermal flux shapes at  $2.5 \times 10^{-3}$  and  $7.5 \times 10^{-3}$  sec. All five approximations, along with the exact result, are represented. The two nodal results are indicated as flux values at the three mesh points. The total inadequacy of the point approximations is again evident. The gross coupling technique appears also to be in serious error. It is a decided improvement on the point method but still yields answers which at certain points are a factor of 100 too small. It provides a surprisingly poor representation of the flux tilt. The  $D/L$  nodal method gives results which are somewhat higher than the adiabatic predictions. They are in error by as much as a factor of 20 at some points. Nevertheless, the method is a major improvement on the point approximation. The synthesis method appears to be the most accurate of those tested. With the three trial functions used for this example a maximum error of 40% results.

Whether or not this intrinsic error is tolerable for any particular transient analysis depends on the self-correcting characteristics of the feedback equations and is hence outside the scope of the present investigation.

Figure 7 displays the analogous results for the 60-cm core. The nodal methods were not tested for this case and the point result at  $t = 10 \times 10^{-3}$  sec is indistinguishable from that at  $t = 0$ . The synthesis method again appears to be the most accurate approximation to the exact solution. In this case it deviates at most 15% from the correct result.

## 2. The Relationship of $T(t)$ to Physical Observables

With the adjoint flux interpreted as neutron importance<sup>11</sup>, Eq. (2) shows that  $T(t)$  represents the integrated importance which all the neutrons

<sup>11</sup>H. HURWITZ, Jr., "Note on the Theory of Danger Coefficients," KAPL-98 (1948).

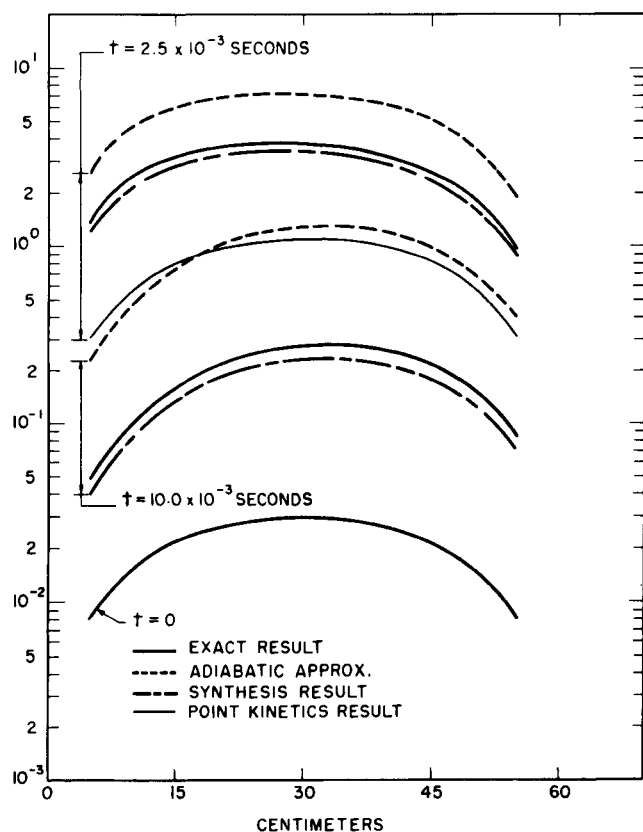


Fig. 7. Prompt critical excursion thermal flux for 60 cm core.

present at time,  $t$ , in the perturbed reactor would have if the reactor had not been perturbed<sup>c</sup>. ( $\psi_1^*$  and  $\psi_2^*$  refer to the *unperturbed critical* reactor.) Frequently in applications involving feedback,  $T(t)$  is interpreted as the normalized power

$$P(t) = \frac{\int [\nu \Sigma_{f1}(x, t) \phi_1(x, t) + \nu \Sigma_{f2}(x, t) \phi_2(x, t)] dx}{\int [\nu \Sigma_{f1}(x, 0) \psi_1(x) + \nu \Sigma_{f2}(x, 0) \psi_2(x)] dx} \quad (17)$$

or as a normalized counter reading

$$R(t) = \frac{\int \Sigma_c(x) \delta(x - x') \phi_2(x, t) dx}{\int \Sigma_c(x) \delta(x - x') \psi_2(x) dx} = \frac{\phi_2(x', t)}{\psi_2(x')} \quad (18)$$

where  $\Sigma_c$  is the cross section for counts of a counter located at  $x = x'$  and assumed to detect thermal neutrons only.

Since functions  $\phi_1(x, t)$  and  $\phi_2(x, t)$  are available, it seems worthwhile to show a comparison of

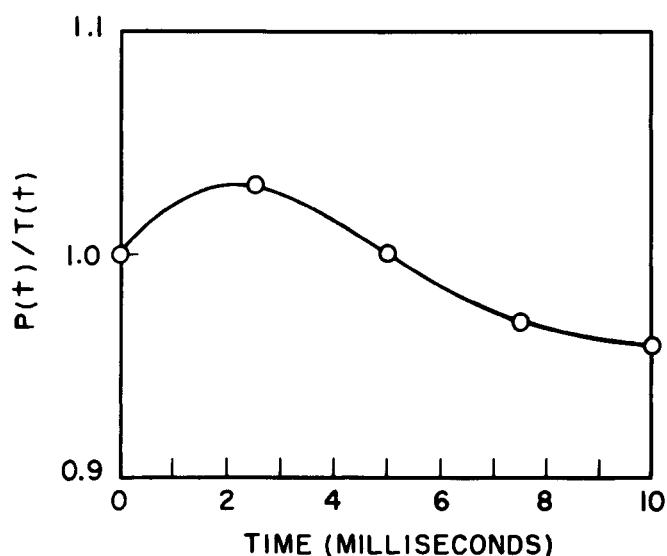
<sup>c</sup>The term  $T(t)$  could of course be defined differently. If, for example, Eq. (1) were weighted respectively by  $\nu_1 \Sigma_{f1}(x, 0)$ ,  $\nu_2 \Sigma_{f2}(x, 0)$ , and  $\nu_1 \Sigma_{f1}(x, 0)$ —instead of  $\psi_1^*$ ,  $\psi_2^*$ , and  $\psi_1^*$ —equations of the form (3) would again result and  $T(t)$ , except for possible time dependence of the fission cross sections, would be identical with  $P(t)$ . However,  $\rho$  and  $\Lambda$  would also have to be redefined, and unless  $\psi_1$  and  $\psi_2$  were known exactly, the computation of  $\rho$  would be subject to greater error.

these three quantities. This is done on Figs. 8 and 9.

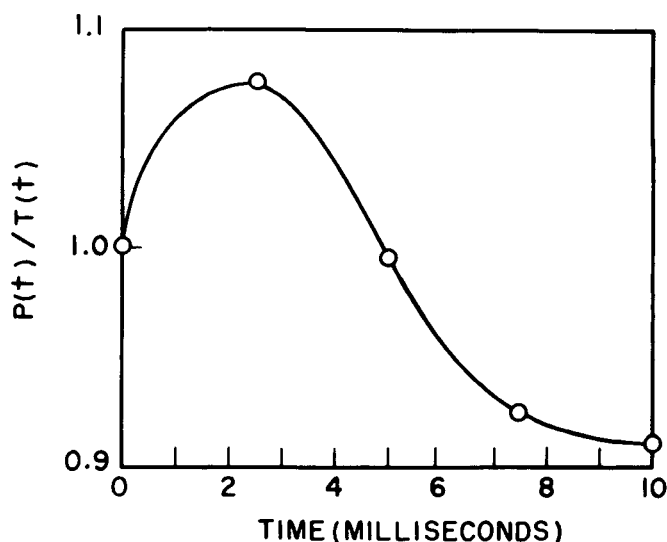
Figure 8 indicates that interpreting  $T(t)$  as being proportional to power level is unlikely to lead to serious error. Even for the large core the ratio is always within 18% of unity.

As might be expected, interpreting  $T(t)$  as a counter reading can lead to significant error. In the extreme example of the 240-cm core,  $R(t)/T(t)$  becomes as small as 1/50. It is perhaps more surprising that even for the 60-cm slab this ratio deviates from unity by as much as 40%.

It should be noted that Figs. 8 and 9 are based on the exact WIGLE solutions. Presumably, the



(a) for a 60-cm core



(b) for a 240-cm core

Fig. 8. Ratio of power to amplitude function (prompt critical problem).

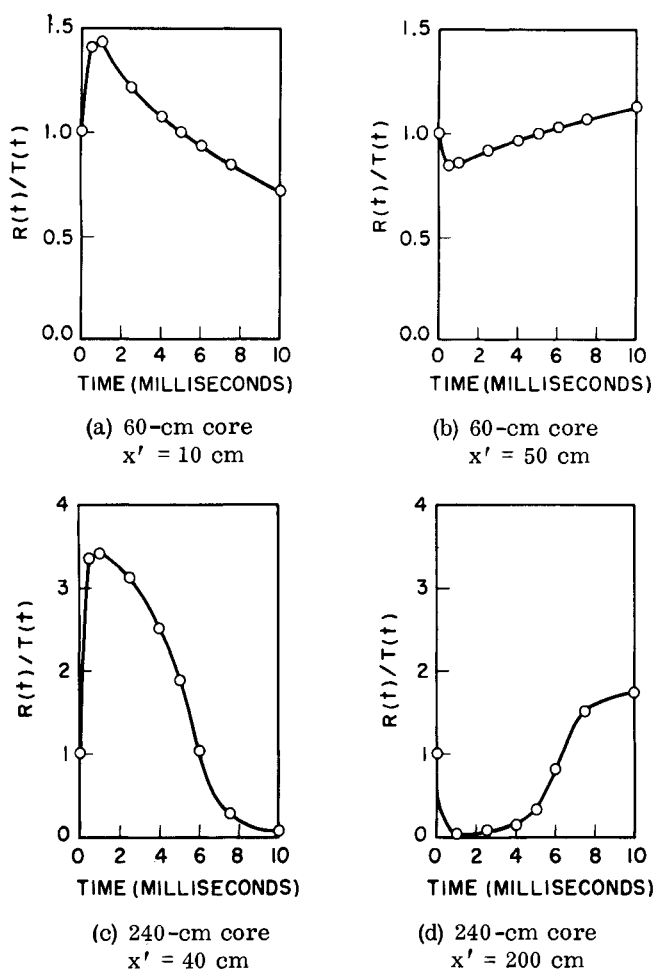


Fig. 9. Ratio of counting rate to amplitude function for prompt critical problem.

adiabatic and nodal approximations would lead to similar curves. Of course, in the point approximation, except for the slight time dependence of the fission cross sections,  $T(t)$ ,  $P(t)$ , and  $R(t)$  are indistinguishable.

### 3. Transient in the Reactivity Range Below Prompt Critical

For relatively slow ramp-type perturbations in the reactivity range below prompt critical, both

inverse velocities may be neglected in solving Eqs. (1). Taking advantage of this fact permitted use of much larger time steps (0.01 sec) in solving the time-dependent diffusion equations in this phase of the study.

As in the prompt critical excursions, exact values of the two-group flux, reactivity, prompt neutron lifetime, amplitude function, and time-dependent shape functions were calculated. These results were again compared with those of the three approximate methods. (The nodal approximation was not investigated for these slower transients.) Two trial functions were again sufficient to describe the 60-cm core behavior by the synthesis method, while a third trial function was necessary for the larger core. The two trial functions in the 60-cm case represented the initial and maximum perturbed states of the core, while the 240-cm core required these two plus a third representing the core at one-half the maximum perturbation.

Table IV shows the values of  $\rho$  and  $T$  at the time (0.8 sec for the large core and 1.0 sec for the small core) when the ramp increase in fission cross section in the first quarter of the core is completed. Exact, point and adiabatic values are listed. In addition, the asymptotic periods at which the fluxes and delayed precursor rise after the ramp insertion has terminated are shown. For this case results of the synthesis method can also be given. Figures 10 and 11 show the exact and approximate flux shapes at the time when the ramp insertion has been completed.

For the large core it is again clear just how unsatisfactory the point kinetics approximation is. The magnitude of the error in both the flux level and the asymptotic period, which stems from the inability of this approximation to account for changes in flux shape, is sizeable. The adiabatic approximation is a definite improvement, especially with regard to its prediction of asymptotic period. The synthesis method yields excellent results.

Only for the ramp excursion applied to the 60-cm core does the point approximation appear to

TABLE IV  
Comparative Results for Ramp Excursion

Method	60-cm core			240-cm core		
	$\rho(1 \text{ sec})$	$T(1 \text{ sec})$	$P_{\text{ASYMP}}(\text{sec})$	$\rho(0.8 \text{ sec})$	$T(0.8 \text{ sec})$	$P_{\text{ASYMP}}(\text{sec})$
Exact	$3.382 \times 10^{-3}$	2.19	11.27	$4.287 \times 10^{-3}$	2.92	4.633
Point Kinetic	$3.200 \times 10^{-3}$	2.03	12.62	$2.560 \times 10^{-3}$	1.71	18.39
Adiabatic	$3.485 \times 10^{-3}$	2.29	10.58	$4.712 \times 10^{-3}$	3.73	4.480
Synthesis	---	---	11.65	---	---	4.650

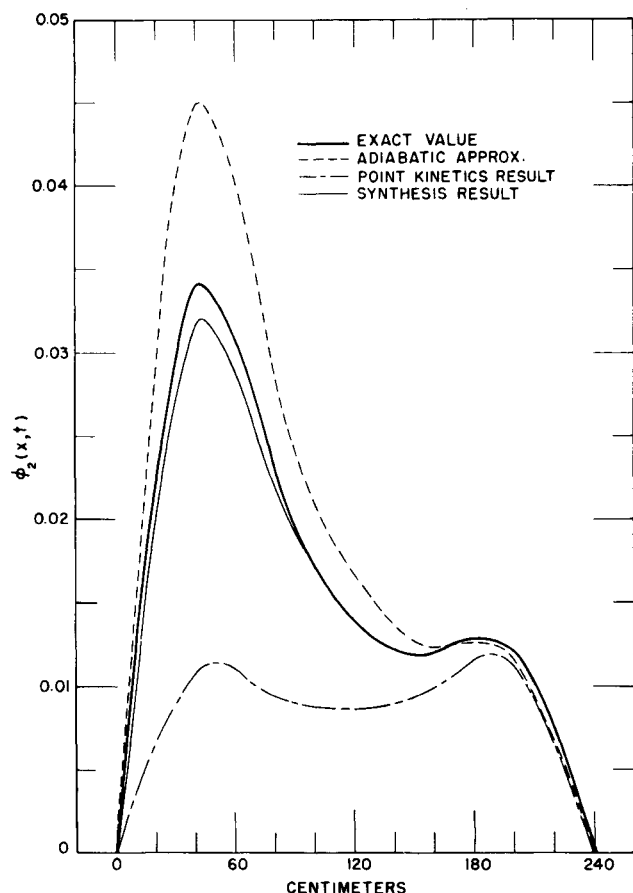


Fig. 10. Delayed critical excursion thermal flux at 0.8 sec for 240 cm core.

be acceptable. (The error in  $T(1 \text{ sec})$  is  $\approx 7.5\%$  and in period  $\approx 10\%$ .) The adiabatic and synthesis approximations are better. (In fact the synthesis and exact flux shapes at  $t = 1 \text{ sec}$  are indistinguishable.) However, in transients encountered during normal power reactor operation the total amount of reactivity present generally is less than  $\beta/2$ . Thus, present results do not indicate any need to abandon the point treatment for description of the transients commonly encountered in the operation of small, tightly coupled power reactors.

#### CONCLUSION

The idealized nature of the cases examined in these numerical experiments prevents any very firm conclusions from being drawn. In particular, since the effects of inherent feedback phenomena have not been accounted for, we have no quantitative feeling for what our results imply for actual reactors. It does seem established, however, that the point kinetics approximation yields a very poor representation of the neutron kinetic behavior when applied to large cores. It is generally recognized that the approximation can be poor. That predic-

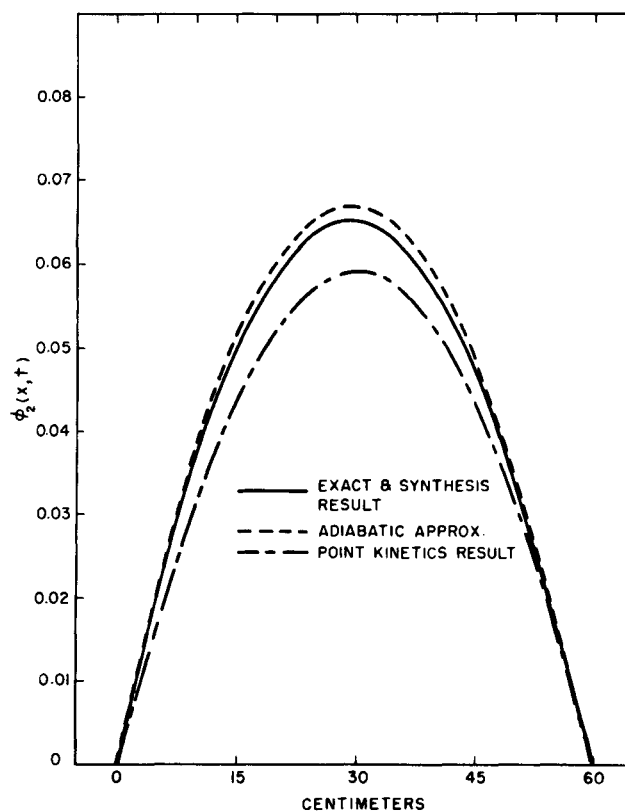


Fig. 11. Thermal flux at 1 sec for 60 cm core.

tions should be off by a factor of more than  $10^4$  was surprising.

Perhaps equally surprising was the magnitude of the inherent inaccuracy of the point model when applied to the prompt critical excursions imposed on the 60-cm slab. With an effective fast-group age of  $\approx 50 \text{ cm}^2$ , this core would generally be considered as fairly tightly coupled. Yet the peak power as predicted by the conventional point model was too small by a factor of  $\approx 4$ , this whole discrepancy evidently being due to the slight change in flux shape associated with the correct space-time solution.

One final conclusion is that for these examples the flux synthesis scheme is definitely the most accurate approximation. It shows promise of being quite satisfactory with the use of only a few trial functions.

#### ACKNOWLEDGMENTS

We wish to thank Prof. Elias Gyftopoulos for helpful discussions carried on when this problem was being defined. Dr. Stanley Kaplan contributed many helpful suggestions concerning application of the synthesis and nodal approximations. Finally, we are indebted to Mr. William G. Clarke who prepared a special experimental computer program for solution of the synthesis equations.